8756 *Inorg. Chem.* **2010**, *49*, 8756–8762
DOI: 10.1021/ic100896a

Inorganic Chemistry
Article

Room-Temperature Synthesis of Nickel Borides via Decomposition of $NaBH_4$ Promoted by Nickel Bromide

Riccarda Caputo,*,† Fabrizio Guzzetta,‡ and Alexander Angerhofer‡

†*ETH Zürich, Department of Chemistry and Applied Biosciences, Lab Inorganic Chemistry, Wolfgang-Pauli Strasse 10, CH-8093 Zürich, Switzerland, and* ‡*Department of Chemistry, University of Florida, Box 117200, Gainesville, Florida 32611*

Received May 6, 2010

We report the formation of nickel borides, at room temperature and pressure, from the decomposition of $NaBH_4$ promoted by the addition of nickel bromide at different concentrations in a dispersing organic medium, tetrahydrofuran and pentane. The nickel borides, formed as amorphous powders, were analyzed, and the structure information served as input for modeling a periodic lattice structure with the same composition. Experimentally, the nickel boride phases were predominantly composed of a boron-rich phase with composition NiB_3. Combining FT-IR, X-ray diffraction analyses, and theoretical structure determination, we suggest for it a monoclinic structure, with symmetry group $P2_1/c$, lattice parameters a =3.038 Å, b = 8.220 Å, c = 5.212 Å, $\alpha = \beta = 90.00°$ and $\gamma = 87.57°$. The enthalpies of formation of the nickel boride phases, as well as the lattice stability, were calculated using density functional theory and density functional perturbation theory methods.

Introduction

It is well-known in the literature that some of the first-row transition-metal salts react, in aqueous or alcohol solutions, with sodium borohydride, to yield finely divided black precipitates, which are active catalysts of the hydrogenation of many organic compounds. In particular, nickel salts (acetate, chloride, sulfate) have been reported to form very active nickel boride catalysts, with compositions Ni_3B and Ni_2B.[1,2] Recently, Ni nanopowder has been used in doping $Zn(BH_4)_2$ reducing greatly the extent of B_2H_6 formed from the thermal decomposition of the zinc borohydride.[3] The hydrolysis of $NaBH_4$ and its use in the generation of hydrogen was already accurately reported by Schlesinger and co-workers and published in the 1950s. In the work published in 1953,[4] the role of anhydrous $CoCl_2$ as a catalytic accelerator of hydrogen release via room-temperature hydrolysis of $NaBH_4$ was reported. Recently, a room-temperature synthesis of nickel borides via hydrolysis of $NaBH_4$ has been reported, and the black precipitate was identified as a crystalline Ni_3B phase.[2] On the other hand, it is well-known since the years when Schlesinger and co-workers started the systematic investigation of complex borohydrides, that the medium in which the reaction takes place, aqueous or alcohol solutions, and the molar ratio between $NaBH_4$ and the nickel salts affect not only the granularity and the crystallinity of precipitates but also the composition. For a long time the exact composition remained unclear, and the black precipitates of nickel borides were generally termed as *nickel borides* catalysts. The room-temperature nickel boride synthesis, and in particular Ni_2B via hydrolysis of alkaline borohydrides, was also reported by Stock[5] some decades ago as a notable synthetic route, since metal borides were otherwise obtained through high temperature reactions. The commercial importance of sodium borohydrides and its derivatives reappeared in the past decade because of its high stoichiometric hydrogen content for possible technological applications in fuel cells and as a reservoir of hydrogen, and has returned the interest toward the use of nickel salts to catalyze the hydrogen release from $NaBH_4$. Therefore, the role of the reaction conditions, as well as the specific transition metal salts used, can help to elucidate the mechanism of hydrogen release and eventually lead a completely reversible process of desorption and absorption of hydrogen for its technological applications. In this paper we report the formation of nickel borides at room temperature and pressure, starting from anhydrous tetrahydrofuran (THF) and pentane dispersions. The amorphous black solid powder formed by the reaction of $NaBH_4$ with Ni(II) salts, namely, $NiBr_2$, at different concentrations

*To whom correspondence should be addressed. E-mail: riccarda.caputo@inorg.chem.ethz.ch.

(1) Paul, R.; Buisson, P.; Joseph, N. *Ind. Eng. Chem.* **1952**, *44*, 1006–1010.
(2) Kapfenberger, C.; Hofmann, K.; Albert, B. *Solid State Sci.* **2003**, *5*, 925–930.
(3) Srinivasan, S.; Escobar, D.; Jurczyk, M.; Yogi Goswami, Y.; Stefanakos, E. *J. Alloys Compd.* **2008**, *462*, 294–302.
(4) Schlesinger, H.; Brown, H.; Finholt, A.; Gilnreath, J.; Hoekstra, H.; Hyde, E. *J. Am. Chem. Soc.* **1953**, *75*, 215–219.
(5) Stock, A. *Hydrides of boron and silicon*; Cornell University Press: Ithaca, NY, 1933.

 Published on Web 09/09/2010

(2.52, 5.46, 7.37, and 10.18% in moles), was studied experimentally by means of FT-IR and X-ray diffraction (XRD), and the composition stated with Rietveld Refinement, in combination with first-principles electronic structure calculations for structure and property determination. In particular, the experimentally determined structural data of Ni−B phases were compared with first-principles structure calculations, to ascertain thermodynamic properties and lattice stability.

Methods

Experimental Settings. $NaBH_4$ was provided by Fisher Scientific and $NiBr_2$ by Acros Organics. Anhydrous pentane and THF were provided by Sigma Aldrich. The XRD instrument (Courtesy to MAIC at the University of Florida) was a Phillips APD 3720; and the FT-IR instrument a 670 FT-IR Nexus Thermo Nicolet EPS. The synthesis we adopted in the present work was a variation of the one reported by Bogdanović and Schwickardi[6] for the synthesis of Ti-doped aluminum hydrides. The powders were weighed in air using an analytical balance (sensitivity ±0.0001 g) and placed in a 25 mL three neck round-bottom flask. Then we added 15 mL of anhydrous THF and pentane. The content of $NaBH_4$ was maintained constant (10 mmol) while the content of $NiBr_2$ was increased for every sample from 2.5 to 10% in moles, exactly (2.52, 5.46, 7.37, 10.18) %. The reaction was performed using anhydrous THF and anhydrous pentane as dispersing medium, since both $NiBr_2$ and $NaBH_4$ are insoluble in those media. The solid state products (powders) were filtered and dried in vacuum. Once dry, the powders were analyzed by means of FT-IR and XRD using the MAUD program[7] for Rietveld refinement. The gas phase, either directly evolved as a product or released upon hydrolysis of the solid phase products (using a NaOH solution, 0.1 M, pH = 13.00, and measured with a thermo Scientific pH meter) was quantified by means of a homemade torricellian manometer filled with water. The number of moles were calculated by the ideal gas equation, $PV = nRT$, where P was the room pressure, corrected by vapor pressure of water at room conditions.

Computational Approach. We used Density Functional Theory (DFT) based methods, in particular CASTEP,[8] as implemented in Materials Studio 5.0 to optimize ionic positions and lattice parameters of α-boron,[9] sodium (bcc), $NaBH_4$, and of all the structures reported in the present work. Norm-conserving pseudo potentials were used for all atoms together with a fine mesh of k-points, with the energy conversion threshold of 0.01 meV/atom, maximum displacement of 0.001 Å and maximum force of 0.03 eV/Å, yielding high accuracy for the energy and atomic displacements. In particular, the number of electrons in the valence region was 3 ($2s^2 2p^1$) for B, 10 ($3d^8 4s^2$) for Ni, 9 ($2s^2 2p^6 3s^1$) for Na, and 7 ($4s^2 4p^5$) for Br. The Perdew−Burke−Ernzerhof 96 and the Generalized Gradient form (GGA-PBE) of the exchange-correlation functional were used. Full geometry optimization was run for all the structures investigated and both internal atomic coordinates and lattice parameters were relaxed. The phonon calculations were performed by using CASTEP Linear Response (DFPT), as implemented in the CASTEP code.[10] A double check of the lattice stability was performed using the Quantum-Espresso code[11] (PWSCF), which is a computer code for electronic-structure calculations within Density Functional Theory and Density Functional Perturbation Theory, using pseudopotentials and a plane-wave basis set. The simulated infrared (IR) spectra were calculated using the property analysis implemented in Materials Studio 5.0, after the phonon calculations performed by using CASTEP. Theoretically, the IR absorption intensities are described in terms of a dynamical matrix, called the Hessian matrix, and the Born effective charges.[12] The Born effective charge tensor was calculated within the linear response formalism, as implemented in Materials Studio 5.0. Reflex powder diffraction module, implemented in Materials Studio 5.0, was used to simulate the XRD patterns of the optimized structures.

Results and Discussion

Nickel Boride Phases. The formation of nickel borides via hydrolysis of $NaBH_4$ promoted by the addition of nickel salts is a well-known process since 1950s, and it has been recently brought to the attention by Albert and coworkers.[2] In the present work we reported a modification of the known synthetic route via hydrolysis, and showed that different nickel boride phases could be obtained using instead organic solvents (THF and pentane), which represented the dispersion medium in which the reaction occurred. The general chemical equation we considered was the following:

$$2NaBH_4(s) + xNiBr_2(s) \xrightarrow[RT]{solv} x\sum_i (Ni,B)_i(s) + 2NaBr(s) + 4H_2(g) \quad (1)$$

where $(Ni,B)_i$ stands for any possible binary solid phase formed by Ni and B, NaBr, was a solid precipitate when the solvent was pentane, or a dispersed solid in THF. The exact mass balance of reaction in eq 1 depended on the number of nickel boride phases formed and their stoichiometry. In principle, different reaction paths for the general chemical equation, eq 1, can be postulated, all depending on the molar ratio of the reactants. Therefore, among all the possible reactions, balanced on the pure stoichiometric requirements, we considered in our theoretical thermodynamic analysis only those reaction paths leading to the formation of those solid phases experimentally suggested of nickel borides, specifically, NiB, nickel-rich phases, with composition Ni_2B, Ni_3B, and one boron-rich phase, NiB_3. For each species on both sides of equation (eq 1), the ground-state structure was determined and the relative thermodynamic stability at finite temperature was ascertained via phonon analysis. Evidently, the maximum theoretical amount of hydrogen gas expected was two mole per mole of $NaBH_4$ used. That is evidently the upper limit of the hydrogen yield because in principle any other thermodynamically allowed compound could bind hydrogen either in the gas phase or in the condensed phase. The former could be diborane and the latter any ternary phase (Ni,B,H), (Na,B,H) and binary phases (Ni,H), (B,H) might be formed under the specific (p, T) conditions. In our theoretical study we did not consider any of those phases because no experimental evidence of them were analytically found. The structural and thermodynamic properties, in particular the enthalpies of formation of the different compounds considered

(6) Bogdanović, B.; Schwickardi, M. *J. Alloys Compd.* **1997**, *253−254*, 1–9.

(7) MAUD stands for Material Analysis Using Diffraction. It is a general diffraction and reflectivity analysis program mainly based on the Rietveld method. It can be downloaded at the following address: http://www.ing.unitn.it/~maud/index.html.

(8) Clark, S.; Segall, M.; Pickard, C.; Haspin, P.; Probert, M.; Refson, K.; Payne, M. *Z. Krystallographie* **2005**, *220*, 567.

(9) Caputo, R.; Züttel, A. *Mol. Phys.* **2009**, *107*, 1831–1842.

(10) Refson, K.; Clark, S.; Tulip, P. **2006**, *73*, 155114.

(11) Plane-Wave Self-Consistent Field: PWscf, Quantum-Espresso. http://www.quantum-espresso.org/.

(12) Baroni, S.; De Gironcoli, S.; Dal Corso, A.; Giannozzi, P. *Rev. Mod. Phys.* **2001**, *73*, 515–562.

Table 1. Calculated Thermodynamic and Structural Data of the Compounds Reported in the Present Work[a]

compound	a, b, c α, β, γ	symmetry group (IT)	$\Delta_f H_0$	remarks
$NaBH_4$	4.359, 4.359, 5.909	$P\bar{4}2_1c$ (114) primitive tetragonal	−251.817[b]	
NiB	3.086, 7.512, 2.992	*Cmcm* (63) centered-orthorhombic	−32.873	for comparison see ref 15
Ni_2B	5.101, 5.101, 4.402	*I*4/*mcm* (140) tetragonal	−59.168	for comparison see ref 15
Ni_3B	5.270, 6.905, 4.559	*Pnma* (62) primitive orthorhombic	−87.284	
NiB_3	3.0381, 8.2204, 5.2123 90.00, 87.57, 90.00	$P2_1/c$ (14) monoclinic	−133.995	

[a] The enthalpies of formation calculated at $T = 0$ K, $\Delta_f H(0)$, are expressed in kJ/mol and the lattice parameters a, b, c, α, β, γ in Å and degrees, respectively. The symmetry group with the IT number, in brackets, was found by searching for the best symmetry representation of the optimized structures within the tolerance of 0.001 Å. The zero point energy and the thermal effects on the enthalpies of formation were not included. The data to be compared are reported in the remark column. [b] In connection to the present work and continuing the work already started in ref 13 other stable structures of $NaBH_4$ have been optimized and modelled following the approach reported for $LiBH_4$ and $Mg(BH_4)_2$ first-principles structure determination. The results are ready to be submitted. For $LiBH_4$ see: Tekin, A.; Caputo, R.; Züttel, A. *Phys. Rev. Lett.* **2010**, *104*, 215501. For $Mg(BH_4)_2$ see: Tekin, A.; Caputo, R.; Sikora, W.; Züttel, A. *Chem. Phys. Lett.* **2009**, *480*, 203.

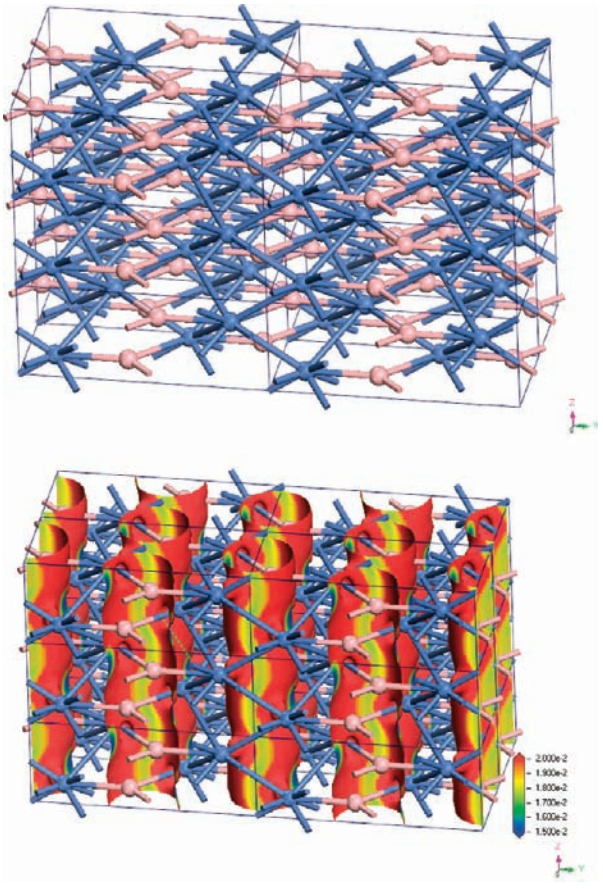

Figure 1. (top) Three-dimensional 2 × 2 × 2 view of the optimized structure of NiB. Representing colors: Ni, blue; B, pink. (bottom) The isodensity surface of the low energy orbital.

in the present work are reported in Table 1. They were calculated as the difference between the total electronic energy of the specific nickel boride compound and the sum of the total energies of Ni and boron. We optimized the structure and calculated the total energy of Ni, face centered cubic structure, and we chose for boron, the α-phase, as reported in ref 9. We considered the primitive tetragonal structure of $NaBH_4$ instead of the face centered-cubic structure [13] because the former showed IR frequencies comparable with the experimental FT-IR spectra, as discussed below. The thermodynamic stability of nickel borides increased with increasing boron content.

(13) Martelli, P.; Caputo, R.; Remhof, A.; Mauron, P.; Borgschulte, A.; Züttel, A. *J. Phys. Chem. C* **2010**, *114*, 7173–7177.

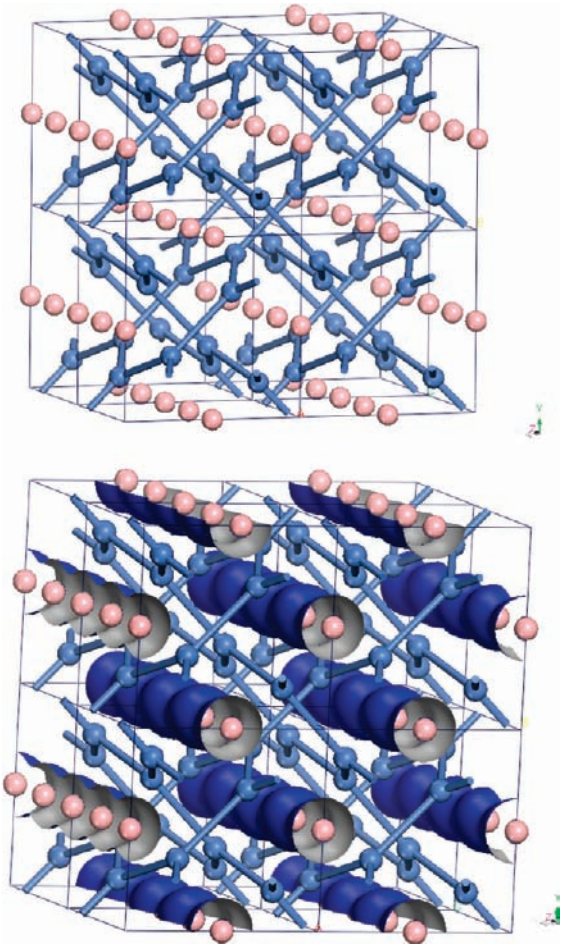

Figure 2. (top) Three-dimensional 2 × 2 × 2 view of the optimized structure of Ni_2B. Representing colors: Ni, blue; B, pink. (bottom) The isodensity surface of the low energy orbital.

In fact, the phase with 75 atom % of boron, NiB_3, was found the most stable one. In terms of a mere structural analysis, the thermodynamic stability directly depended on the possibility of forming boron cluster-based structures. The centered-orthorhombic structure of NiB, 50 atom % of boron, was formed by hexagonal-based layers, alternatively occupied by Ni and B atoms, as shown in Figure 1, where the Ni−B bond length was 2.192 Å. The boron atoms, aligned along the $\vec{c}$-direction in a zigzag arrangement, were 1.749 Å apart. The electron density distribution clearly showed the spreading of p-type orbitals across the boron atoms, and an overlapping with the

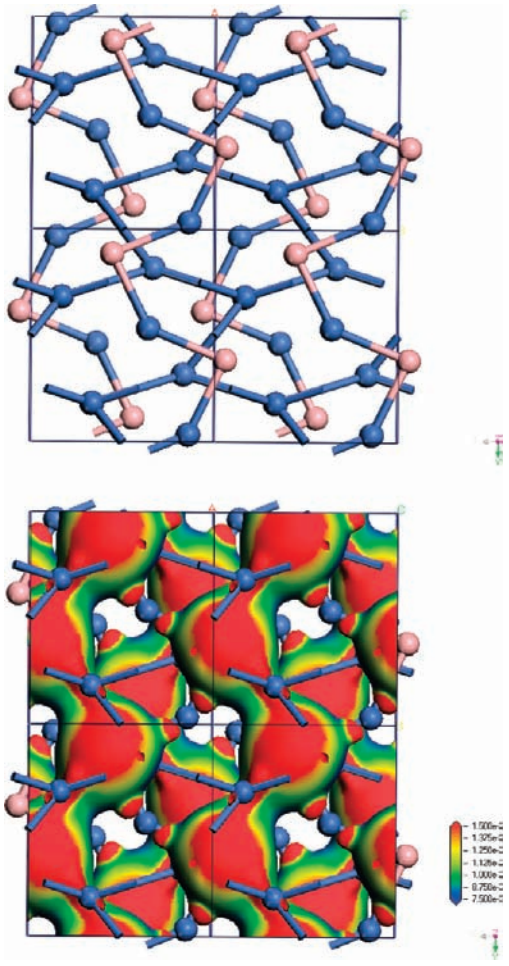

Figure 3. (top) Three-dimensional 2 × 2 × 2 view of the optimized structure of Ni_3B. Representing colors: Ni, blue; B, pink. (bottom) The isodensity surface of the low energy orbital.

d-states of Ni. In particular, the orbitals in the energy range [−5.02, −3.62] eV extended over Ni and B atoms along the $\vec{c}$-direction. While the orbitals at low energy, namely, [−12.53, −9.11] were responsible for the B−B p-type orbital overlapping along the zigzag chain in the $\vec{c}$-direction, as shown in Figure 1. Similarly, Ni_2B showed a linear alignment of boron atoms along the $\vec{c}$-direction, with bond length of 2.201 Å and the nickel atoms formed orthogonally arranged hexagonal layers, as shown in Figure 2, in which Ni−Ni bond lengths on each hexagon were all equal to 2.474 Å. The low energy states in the range [−11.42, −9.45] eV were assigned to the p-type orbital overlapping along the boron chain as shown in Figure 2. In Ni_3B, the boron atoms did not form a linear chain, but a zigzag-like chain along the $\vec{b}$-direction formed alternatively by one Ni and one B atom, immersed in a sublattice of nickel atoms, as shown in Figure 3. For that composition the low energy orbital [−10.07, −8.48] eV extended along the zigzag chain and mainly localized on boron atoms. Interestingly, the structure of the boron-rich phase, namely, NiB_3, again showed the typical linear motif of boron chains clustering in the metal lattice. As reported in Figure 4, the three linear boron chains extending along the $\vec{b}$-direction, shared the lowest energy orbital at −16.039 eV. A more careful analysis of the orbital distribution revealed that up to energy level of

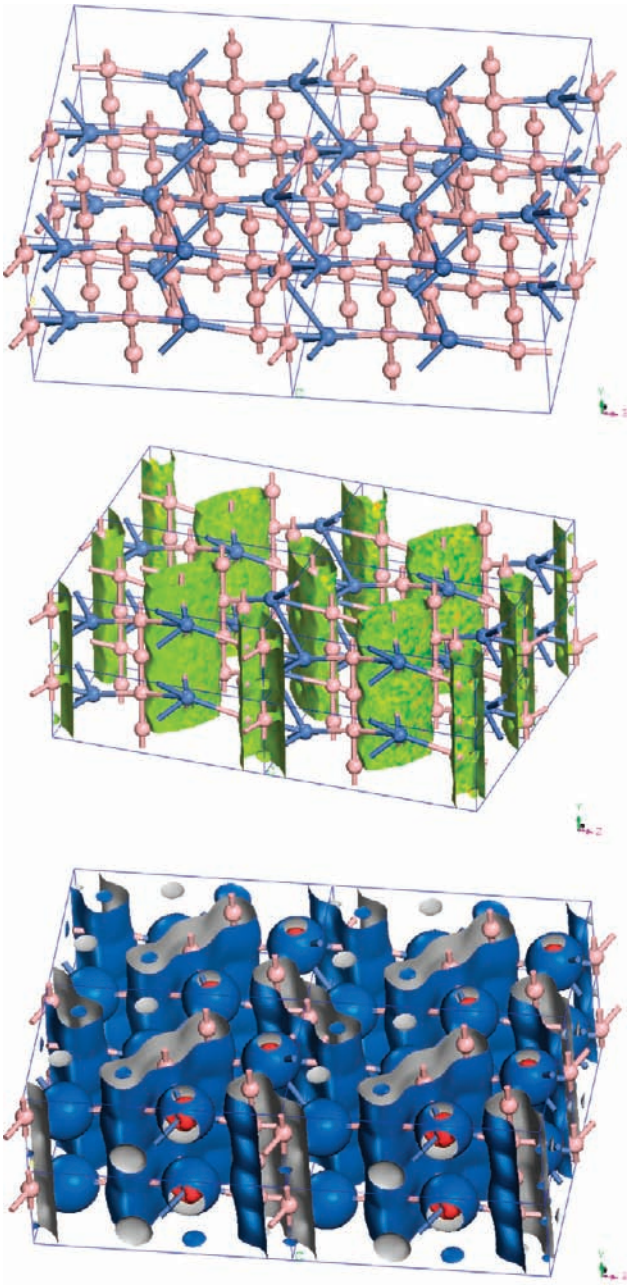

Figure 4. (top) Three-dimensional 2 × 2 × 2 view of the optimized structure of NiB_3. Representing colors: Ni, blue; B, pink. (center) The isodensity surface of the low energy orbital. (bottom) The total electron density isosurface at 0.45 $Å^{-3}$.

−4.651 eV, the electronic states described the electron distribution between those three linear chains (the green isosurface). The next higher electronic state at −2.714 eV (the blue isosurface) clearly described the d-type orbital localized on nickel atoms. A comparison of the total electron density of states of elemental Ni with the nickel borides phases, reported in the present work, is shown in Figure 5. The electronic structure of transition metal borides, and in particular nickel borides, have been discussed since very early, when Kiessling[14] in the mid of 1940s started a systematic investigation of binary systems between transition metals and boron. In one of his

(14) Kiessling, R. *Acta Chem. Scand.* **1950**, *4*, 209–227.

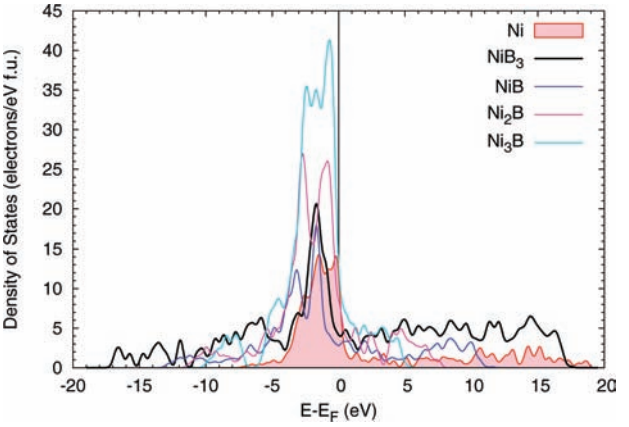

Figure 5. Total electron density of states of elemental Ni compared with NiB, Ni_2B, Ni_3B, NiB_3.

papers[14] he discussed the question of the electron transfer in borides with boron chains, and concluded, on the basis of the experimental evidence, that Pauling's theory was rebutted, as the electron transfer from the chains to the metal lattice occurred. Our analysis of the total electron density difference of the nickel boride phases investigated in the present work, confirmed that electron charge accumulates on the nickel side, while boron experiences a charge depletion in favor of a certain amount of charge accumulation along the boron chains, as shown in Figure 6. The calculated XRD patterns of nickel borides phases are reported in Figure 7, compared to the XRD pattern of the $NaBH_4$ tetragonal phase. Clearly, the peaks at 2θ = 19.87 and 29.95 degrees were characteristic of the NiB_3 phase because none of the nickel-rich phases, namely, Ni_xB, for x = 1, 2, 3, showed a diffraction in that region. Instead, the diffraction peaks in the range [40, 50] were common with all the nickel boride phases investigated. A confirmation that those two characteristic diffraction ranges could be attributed to NiB_3 derived from the experimental XRD spectra performed after hydrolysis of the nickel boride powder, as shown in Figure 9. The XRD of the samples (both in THF and in pentane) with the 10.18 mol % of $NiBr_2$ taken before and after the hydrolysis of the nickel boride powders showed that the results were almost the same and also that the powder we formed this way was amorphous. The XRD, using Kapton tape (C.S. Hyde Company) as protective medium, showed the peaks of unreacted $NaBH_4$ in the powders, which disappeared after its hydrolysis. The Rietveld analysis of the whole solid state product of the direct reaction gave as predominant phase a nickel boride with atomic ratio 1:3 Ni:B and orthorhombic structure. The weight % of such a phase ranged from 90 to 99% of the total solid state products. By performing total energy calculations via full geometry optimization of the experimental orthorhombic structure, the lowest energy state was reached when the structure changed to monoclinic. The main structural difference between the orthorhombic and the monoclinic structures was found in the alignment of one of the boron chains, which was zigzag-shaped in the orthorhombic case and linear in the monoclinic. Interestingly, the latter resulted stable with no imaginary

(15) Sato, S.; Kleppa, O. **1982**, *13*, 251−257.

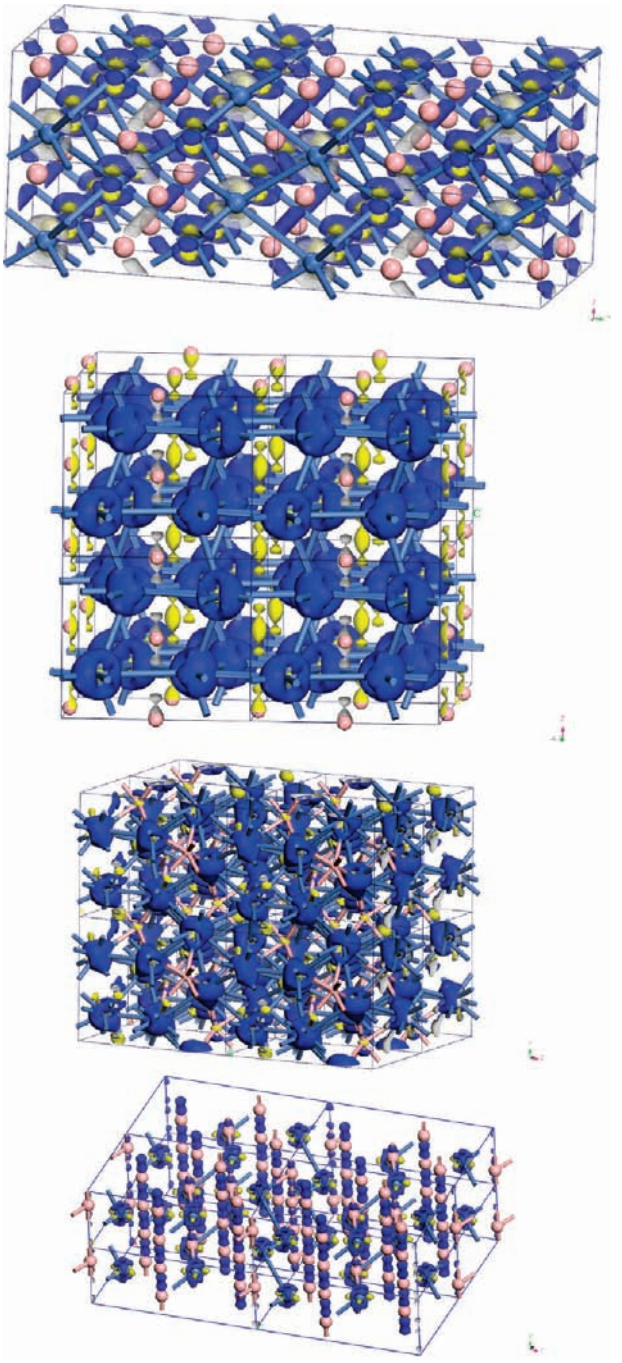

Figure 6. (top to bottom) The electron density difference of NiB, Ni_2B, Ni_3B, and NiB_3. The isodensity surfaces are at the following values: 0.012, 0.045, 0.045, 0.040 electrons $Å^{-3}$. Representing color: charge accumulation regions, blue; charge depletion regions, yellow.

modes in the phonon calculations. The orthorhombic structure showed symmetry group *Pnma* (IT 62) and lattice parameters *a*, *b*, *c* equal to 5.694 Å, 3.275 Å, 7.226 Å. Instead, one of the lattice angles of the monoclinic structure differed from the 90° value of only 2.43°. Clearly, the linear alignment of boron atoms lowered the total energy and led to a gain in lattice stability, as the enthalpy of formation at T = 0 K passed from +46.156 kJ/mol of the orthorhombic structure to −133.995 kJ/mol of the monoclinic structure. Therefore, because the experimental XRD patterns could only show the dominant diffraction peaks, because of powder phases formed, we suggested on the

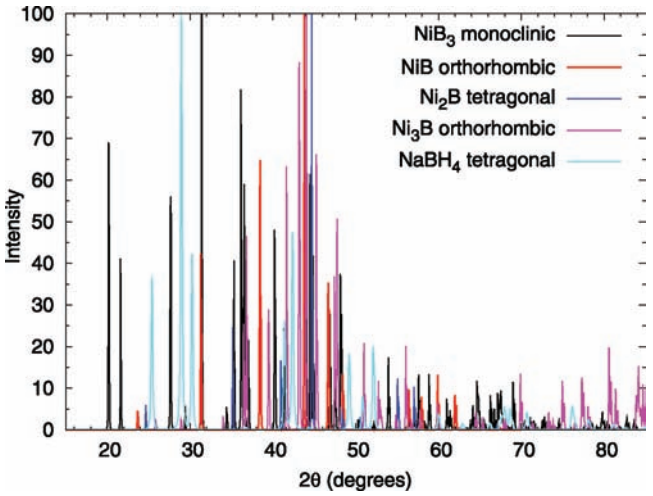

Figure 7. Simulated XRD diffraction patterns of NiB, Ni_2B, Ni_3B, NiB_3 compared with the corresponding pattern of $NaBH_4$ tetragonal structure.

Table 2. Fractional Coordinates of the Boron-Rich Structure, Namely, NiB_3 Monoclinic[a]

ion type	*x*	*y*	*z*
B	0.015	0.359	0.278
B	0.486	−0.359	−0.278
B	0.250	0.000	0.000
Ni	0.278	0.393	0.863

[a] The reported atomic coordinates were obtained after full geometry optimization of the experimentally determined structure, used as input in the DFT calculations, and then fitted with the monoclinic symmetry group, $P2_1/c$, which best represented the optimized structure.

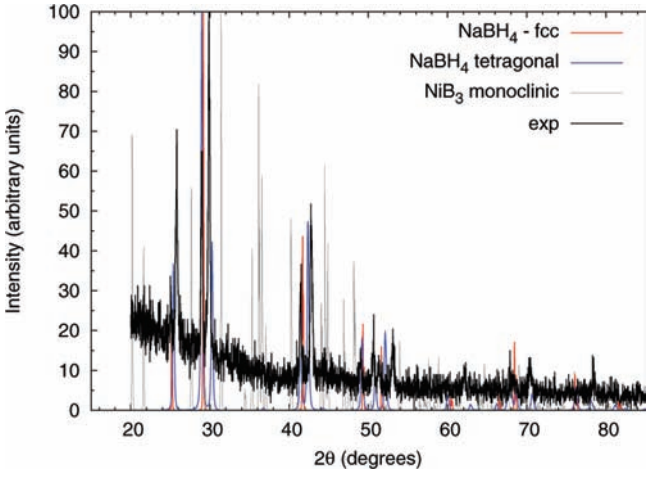

Figure 8. Experimental (black) XRD pattern of the solid state products obtained by the direct reaction (eq 1) with adding 10.18 mol % of $NiBr_2$. For comparison, we reported the simulated XRD patterns of $NaBH_4$, cubic and tetragonal structures, red and blue lines, respectively, together with the corresponding XRD pattern of the modeled structure of NiB_3.

basis of the first-principles structure determination that the crystal stable phase was the monoclinic structure of NiB_3 (Table 2). Intense work on improving the crystallinity of the novel boron-rich phase is still in progress. The Figure 8 and Figure 9 showed the experimental diffraction patterns of the powder directly formed by adding 10.18 mol % of $NiBr_2$ and after its hydrolysis, respectively. For the sake of clarity, we overlapped the simulated XRD patterns of $NaBH_4$ and NiB_3 with the experimental ones

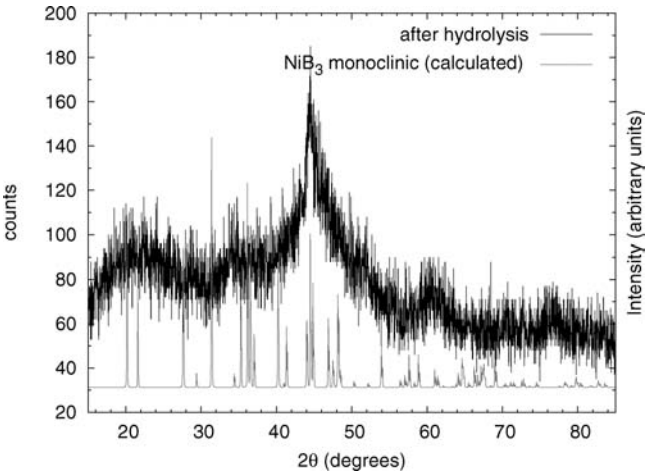

Figure 9. Experimental (black, left scale) XRD pattern of the nickel boride phases obtained after the hydrolysis of the solid state products of reaction in eq 1 with addition of 10.18 mol % of $NiBr_2$. For comparison, (gray, right scale) we overlaid the simulated XRD pattern of the modeled structure of NiB_3. The hydrolysis helped to clean the sample from water-soluble unreacted reagents, namely, $NaBH_4$ and $NiBr_2$. The nickel boride phases were clearly amorphous.

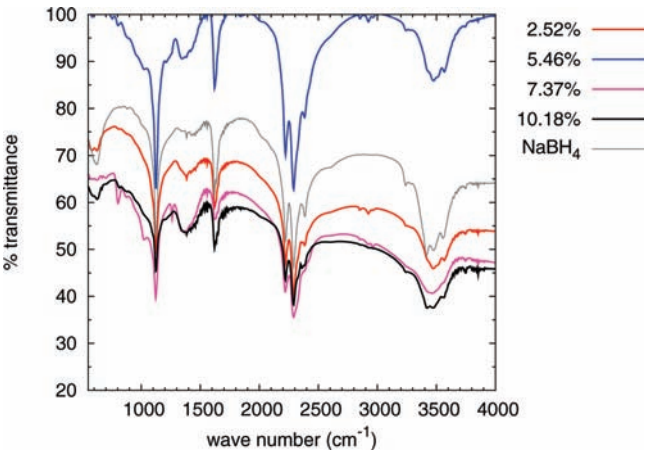

Figure 10. FT-IR spectra of the pentane-synthesized solid products of reaction in eq 1 at different concentrations of $NiBr_2$. For comparison the FT-IR spectrum of the pure $NaBH_4$ was reported.

in Figure 8. Although the intrinsic difficulties to obtain sharp diffraction peaks, because of powder formed with very low crystallinity, in the XRD pattern in Figure 8 the characteristic peaks of the dominant nickel boride phase, NiB_3, were identified at $2\theta = 20°$, 30°, and 41°. Those diffraction peaks become broad after the hydrolysis, as shown in Figure 9. A systematic study to improve the crystallinity of the novel boron-rich phase is still in progress. We obtained a confirmation that the composition of nickel boride phases formed did not depend on the particular dispersing medium used by performing the FT-IR spectra. The experimental FT-IR spectra (KBr pellets) of the solid state products of reaction, reported in Figure 10, showed an increasing broad signal in the wavenumber range 1300−1400 cm^{-1} with increasing content of nickel bromide. The two concentration-independent frequencies in the range of 1600−2200 cm^{-1} were also present after hydrolyzing the solid phase product, as shown in Figure 11. Clearly, they could be attributed to neither $NaBH_4$ nor $NiBr_2$. In fact, the frequency at 1120 cm^{-1} in

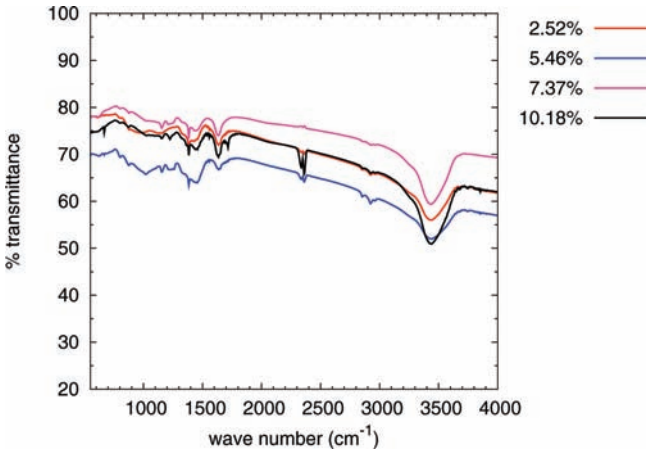

Figure 11. FT-IR spectra of the pentane-synthesized powders after hydrolysis at different concentration of $NiBr_2$.

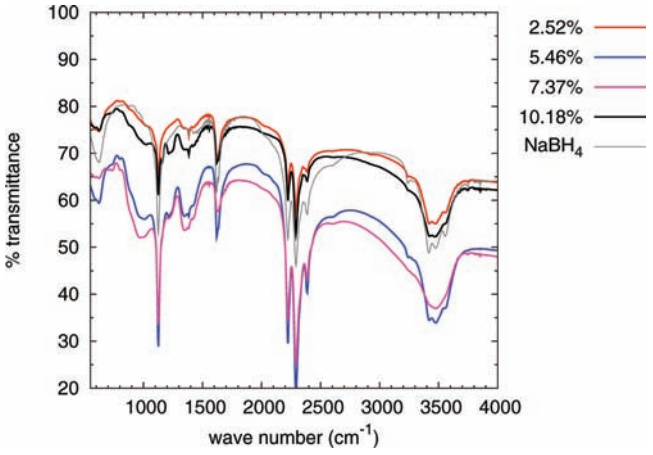

Figure 12. FT-IR spectra of the medium-free mixture of reactants, $NaBH_4$ and $NiBr_2$, at different concentration of the latter component.

Figure 10, which intensity decreased as the nickel content in the reactants increased, was due to the bending mode of the $NaBH_4$ tetragonal phase. It disappeared after the hydrolysis of the nickel boride phases. Interestingly, we repeated the FT-IR measurements without adding any dispersing medium. The broad band with wave numbers in the range 1300−1400 cm^{-1} was still present, as shown in Figure 12, confirming that a solid state reaction occurred. The phonon calculations of nickel boride phases, in particular, NiB and NiB_3, that we chose for comparison confirmed that the low wavenumber broad band, experimentally measured, coincided with the calculated phonon frequencies of NiB_3, monoclinic structure. In fact, the calculated phonon frequencies of NiB fell in a lower range of wave numbers. We rationalized the different phonon frequencies of the two phases, by means of structural differences between them. In NiB, boron atoms did not form any chain, while in NiB_3, the linear chains enabled the stretching modes of boron atoms, with wave numbers in (1265,1296) cm^{-1}, as reported in the Supplementary Data.

Gas Phase Analysis. The amount of gas produced was quantified in situ during the reaction and when it was over during the hydrolysis of the whole solid phase recovered in the products, as reported in Table 3. The evolution of the gas during the reaction increased exponentially with increasing quantity of nickel bromide in the reactants. The amount of gas coming from the hydrolysis of the nickel boride powders showed a maximum yield in the case of the powder formed by using 5.46 mol % of $NiBr_2$.

Table 3. Quantitative Analysis of the Gas Phase Developed in the Reaction of Equation 1[a]

$NaBH_4$	$NiBr_2$	$NiBr_2$	direct synthesis		after hydrolysis	
mg	mg	% mole	V_{gas}/mL	$mmol_{gas}$	V_{gas}/mL	$mmol_{gas}$
383.8	56.1	2.52	20	0.85	46	1.78
374.7	118.1	5.46	36	1.55	64	2.48
386.6	164.8	7.37	62	2.58	22	0.87
375.0	220.0	10.18	106	4.49	42	1.66

[a] We report the weighed quantities in mg of the reactants, the corresponding % mole of $NiBr_2$, the volume of gas evolved directly from the reaction and after the hydrolysis of the solid state products at pH = 13.00 (0.1 M NaOH).

Conclusions

The main focus of the present work was the possibility to synthesize nickel borides not only via hydrolysis of $NaBH_4$ and adding nickel salts, as already known, but by using organic solvents (THF and pentane) as dispersing medium. In addition, the quantitative analysis of the gas phase, showed the possibility to release considerable amount of hydrogen at (p,T) room conditions. The FT-IR of nickel boride phases (in particular those obtained from the 10% of $NiBr_2$ after being hydrolyzed) either prepared using THF or pentane showed the possibility to form the same products, since no other vibrations in the spectrum were observed. The combined theoretical and experimental study of the reaction products led to the identification of a novel boron-rich phase with composition NiB_3, to our knowledge not yet known and reported. Preliminary qualitative analyses of the gas phase showed that it was predominantly formed by hydrogen. No appreciable quantities of diborane were detected. In addition, the hydrolysis of nickel boride phases released an additional amount of hydrogen, clearly suggesting the presence of residual $NaBH_4$ unreacted in the direct reaction. Therefore, it is very unlikely that the general reaction (eq 1) could lead to the formation of diborane, being that the mole of boron quantitatively bound all in the solid phase. The present work highlighted on the one hand an alternative synthetic route to nickel borides, mainly dominated by the new boron-rich phase, NiB_3; and on the other hand showed the possibility to produce hydrogen at room conditions, which is of particular interest in fuel cell applications. $NaBH_4$ alone, in fact, did not release hydrogen in the same solvent and (p,T) conditions.

Acknowledgment. R.C. gratefully acknowledges the financial support from the European Commission DG Research RTN Marie Curie Actions-Hydrogen (contract MRTN-CT-2006-032474, until February 2009) and the 7. Serie Interner F+E-Projekte, EMPA funding. The computer facilities IPAZIA at EMPA in Dübendorf, Switzerland are highly appreciated (http://ipazia.empa.ch). F.G. is pleased to acknowledge the MAIC (Major Analytical Instrumentation Center) for the XRD instrumentation. We thank A. Masello for his assistance with the FT-IR spectrometer and W. Imaram for useful advice.

Supporting Information Available: Results of the calculations of the NiB_3 phonons. This material is available free of charge via the Internet at http://pubs.acs.org.